Materials dependence of the spin-momentum transfer efficiency and critical current in ferromagnetic metal/Cu multilayers

M. R. Pufall, W. H. Rippard, and T. J. Silva
National Institute of Standards and Technology, Magnetic Technology Division 816.01, 325 Broadway, Boulder, Colorado 80305

(Received 10 March 2003; accepted 7 May 2003)

We have quantitatively compared spin-momentum transfer effects in FM/Cu multilayers, with FM=Co, $Co_{90}Fe_{10}$, $Ni_{80}Fe_{20}$, $Ni_{40}Fe_{10}Cu_{50}$, and Fe. All of the measured multilayers exhibited an abrupt step up in resistance at a critical current I_c, the value of which was a linear function of applied magnetic field H_{app}. The spin-transfer efficiencies determined from these data were in substantial agreement with their predicted values over the range of materials studied. $I_c(H_{app})$, when evaluated at zero net field, was found to increase with the exchange energy density of the ferromagnet, demonstrating the tunability of the critical current by materials selection.
[DOI: 10.1063/1.1590432]

A substantial body of recent research has examined the torque exerted on a magnetic material by an incident spin-polarized electric current, an interaction known as the spin-momentum transfer (SMT) or spin-torque effect.[1] Interest in SMT is driven in part by the fact that SMT provides a means of manipulating magnetic materials without using external magnetic fields. Research has primarily focused on observation of SMT in a variety of geometries that facilitate the high current densities (10^7 A/cm^2) required for the effect.[1] However, the majority of work to date has studied the Co/Cu material system: very little has been reported on current-induced effects in other material systems.[2,3] Those experiments that have employed materials other than Co/Cu have used geometries sufficiently different that little can be deduced about the role of the materials' magnetic properties.[2–4]

In this letter, we report the observation and analysis of current-induced magnetic excitations in multilayer samples grown from a range of magnetic materials, while keeping Cu as the nonmagnetic spacer layer. As in our previously reported work on the Co/Cu system,[5] measurements were performed using a mechanical point-contact measurement system. For the multilayer systems discussed here, we observe a step in the dc resistance and a corresponding peak in the differential resistance (dV/dI) at a critical current I_c, when measured in a large out-of-plane applied field $H_{app} > M_{eff} - H_{ex}$, where M_{eff} is the effective saturation magnetization density (reduced by surface anisotropy from the bulk saturation value M_s) and H_{ex} is the effective interlayer exchange field. For all materials studied, this step in resistance is reversible (anhysteretic), and I_c is a linear function of H_{app}. To analyze these data, we use the theory developed by Slonczewski.[6] This theory ascribes the step in resistance at I_c to the onset of coherent magnetization precession and spin-wave generation in the top magnetic layer in the multilayer. The extracted spin-transfer efficiencies ε of the various ferromagnetic (FM) materials are in reasonable agreement with predicted values. Furthermore, we find that the absolute values of I_c can be controlled by varying the exchange stiffness properties of the FM layer, in agreement with the predictions of Ref. 6. Independent of this theory, the increase of I_c with exchange stiffness suggests that a spatially nonuniform magnetization is induced by the current. Indeed, recent measurements have directly shown that magnetization dynamics are excited by a dc current in both nanopillars[7,8] and lithographic point contacts.[8]

We studied multilayered thin-film samples grown at the first antiferromagnetic interlayer exchange-coupling maximum. The films were of the form Fe(5.0 nm)/{Cu(0.9 nm)/FM(1.2 nm)}×10/Cu(1.0 nm), in which FM=Co, $Co_{90}Fe_{10}$, $Ni_{80}Fe_{20}$, Fe, and $Ni_{40}Fe_{10}Cu_{50}$, sputter-deposited onto oxidized Si. Diluting $Ni_{80}Fe_{20}$ with Cu provides a controlled means of decreasing both the saturation magnetization M_s and the exchange stiffness D of the material, allowing study of a material with markedly different exchange properties.[9] The 5.0-nm Fe bottom layer is a seed layer for growth. Values for H_{ex} and M_{eff} were determined from measurements of the giant magnetoresistance for both in-plane and out-of-plane applied field, in conjunction with alternating-gradient magnetometry and superconducting quantum interference device (SQUID) magnetometry measurements. The damping parameter α_{LLG} was obtained from ferromagnetic resonance and pulsed-inductive microwave magnetometry measurements. The values of the measured parameters fell within the ranges reported in the literature.

The mechanical point-contact system used to produce the high current densities necessary for SMT is similar to those described elsewhere.[10] The tip material used was Ag. For contact stability, measurements were made at temperatures ranging from 5 to 6 K. Fields up to 6 T were applied perpendicular to the sample plane, to conform to the geometry modeled by Slonczewski. Contact resistances in the range from 15 to 150 Ω were typically obtained, with higher resistance contacts having a greater probability of showing SMT effects. The dc and differential resistance were measured as a function of current through the tip and applied magnetic field to determine $I_c(H_{app})$, and a series of contacts made to each type of multilayer film to obtain statistics I_c.

Shown in Fig. 1(a) is a representative set of differential resistance curves, taken at several values of H_{app}, for a contact made to a $Co_{90}Fe_{10}$/Cu multilayer. The peaks seen in the

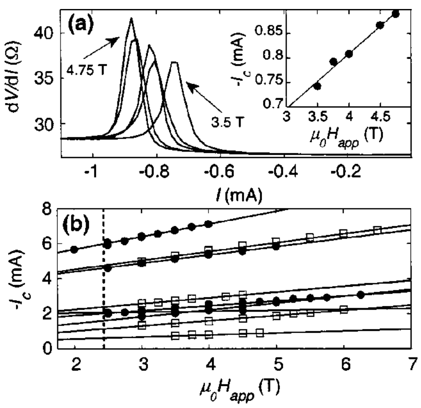

FIG. 1. (a) dV/dI vs I and $\mu_0 H_{\mathrm{app}}$ for $\mathrm{Co_{90}Fe_{10}}$/Cu multilayers. Inset: I_c vs $\mu_0 H_{\mathrm{app}}$ extracted from the data for dV/dI vs I. The range of applied field for each contact varied according to the stability of the contact and the persistence of the peak in the dV/dI at low fields. (b) I_c vs $\mu_0 H_{\mathrm{app}}$ for a series of contacts to $\mathrm{Co_{90}Fe_{10}}$/Cu multilayers. Vertical dotted line indicates applied field for zero net field in the magnetic layers, $H_{\mathrm{app}} = M_{\mathrm{eff}} - H_{\mathrm{ex}}$.

dV/dI signal, which identify I_c, occur for only one direction (negative) of current flow. This corresponds to electrons flowing from the tip into the sample and is a signature of SMT.[11] The inset to Fig. 1(a) shows the linear dependence of I_c on applied field. Both the slope and intercept of the line I_c versus H_{app} varied from contact to contact, resulting in a set of lines $I_c(H_{\mathrm{app}})$, shown in Fig. 1(b) for the $\mathrm{Co_{90}Fe_{10}}$/Cu multilayer. Similar sets of data were obtained for each of the other materials. As seen in Fig. 1(b), peaks sometimes persisted for $H_{\mathrm{app}} < M_{\mathrm{eff}} - H_{\mathrm{ex}}$, but not consistently. Analysis was limited to data taken with $H_{\mathrm{app}} > M_{\mathrm{eff}} - H_{\mathrm{ex}}$.

Slonczewski derived a relation for systems in which the magnetization M and current density J are perpendicular to the plane of the sample.[6] It is assumed that the magnetization of the top layer of the multilayer is "free;" i.e., it can react to spin torque applied by the current, and that the buried layers act as a "fixed" magnetic layer. The spin currents in this structure exert a torque on the free layer and induce precessional motion of M in the region under the tip. A modified Landau–Lifshitz–Gilbert (LLG) equation that includes a spin-torque drive term is used to model the dynamics. The torque induced by the spin current is damped by both the conventional LLG viscous damping and by spin-wave radiation away from the tip. The onset of precessional motion of M occurs when the current-induced torque equals the damping torque. This results in the expression

$$I_c(H_{\mathrm{app}}) = \frac{e t_1}{\hbar \varepsilon}\left[\frac{23.4 M_s D}{2\hbar\gamma} + 6.3 r^2 \alpha_{\mathrm{LLG}} M_s (H_{\mathrm{app}} + H_{\mathrm{ex}} - M_{\mathrm{eff}})\right], \tag{1}$$

in which D is the spin-wave exchange stiffness, t_1 the magnetic layer thickness, e the electron charge, ε the efficiency of spin current conversion to torque, α_{LLG} the LLG damping parameter, r the contact radius, γ the gyromagnetic ratio, M_s the bulk saturation magnetization, and M_{eff} the effective magnetization including surface anisotropy. The first term in Eq. (1) results from spin-wave radiation and the second from the intrinsic damping of the material.

Evaluating Eq. (1) at the field $H_{\mathrm{app}} = M_{\mathrm{eff}} - H_{\mathrm{ex}}$ yields

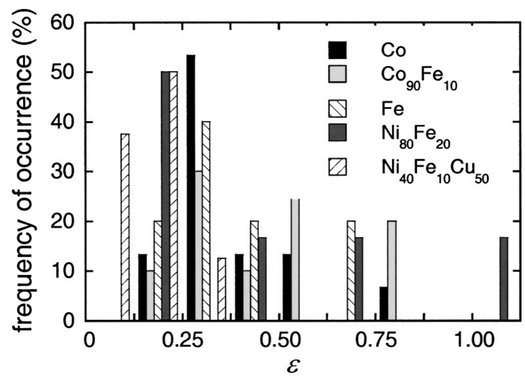

FIG. 2. Distributions of determined values of ε, for each material studied. Bin size on ε is 0.125.

$$I_c^* \equiv I_c(H_{\mathrm{app}} = M_{\mathrm{eff}} - H_{\mathrm{ex}}) = \frac{e t_1}{\hbar \varepsilon}\left(\frac{23.4 M_s D}{2\hbar\gamma}\right). \tag{2}$$

This expression is a function of known material parameters M_s, D, t_1, and the yet-to-be-determined efficiency ε, and is independent of the contact size. By inverting this relation, we determine ε for an individual contact. A series of point-contact measurements, each exhibiting results qualitatively similar to Fig. 1(b), was made and analyzed for each material system. The resulting distributions for ε are shown in Fig. 2, with the data summarized in Table I. The distributions are qualitatively similar for the different materials, each showing a maximum in the range 0.2 to 0.4. From log-normal fits to the distributions (since $\varepsilon \geqslant 0$) we found the maxima in probability to occur at $\varepsilon = 0.36$, 0.40, 0.35, 0.26, and 0.28 for Co, $\mathrm{Co_{90}Fe_{10}}$, Fe, $\mathrm{Ni_{80}Fe_{20}}$, and $\mathrm{Ni_{40}Fe_{10}Cu_{50}}$, respectively. The fitted widths (defined as plus/minus one standard deviation) are given in Table I.

The value of the angular momentum transfer efficiency depends on the nature of the point contact and the consequent electron transport. In the limit of ballistic transport, ε depends on the degree of spin polarization of the material P: $\varepsilon = 2[(P^{1/2} + P^{-1/2})^3 - 4]^{-1}$. For a 100% polarized material, $\varepsilon = 0.5$. For a typical ferromagnet such as Co, $P \approx 0.45$, and $\varepsilon \approx 0.28$.[12,13] For diffusive transport, ε is a function of the spin-dependent resistivities $\rho_{\uparrow/\downarrow}$ of the material, with a lower bound predicted as $\varepsilon_{\mathrm{diff}} > (\rho_\downarrow - \rho_\uparrow)/2(\rho_\downarrow + \rho_\uparrow)$. For Co, $\varepsilon_{\mathrm{diff}} \approx 0.2$–$0.25$.[14] In practice, ε will vary from contact to contact, since the contact dimensions are intermediate between the ballistic and diffusive regimes. The expected ranges for ε are shown in Table I, calculated using literature values of

TABLE I. Magnetic properties, and theoretical and determined efficiencies of materials studied. Theoretical limits on ε given by ballistic "(b)" and diffusive "(d)" models. M_s values from Ref. 17, D values determined from Ref. 18, except $\mathrm{Ni_{80}Fe_{20}}$ and $\mathrm{Ni_{40}Fe_{10}Cu_{50}}$ by Brillouin light scattering. Polarization values for ballistic ε from Refs. 12 and 13, spin-dependent resistivities for diffusive ε from Refs. 14, 15, and 16.

	$\mu_0 M_s$ (T)	D (meV nm^2)	A (pJ/m)	Fitted ε range	Theoretical ε range
Co	1.80	5.00	28.5	0.29–0.44	0.21(d)–0.31(b)
$\mathrm{Co_{90}Fe_{10}}$	1.84	4.78	29.2	0.29–0.56	0.30(d)–0.37(b)
Fe	2.18	2.81	20.2	0.27–0.47	0.34(b)–0.42(d)
$\mathrm{Ni_{80}Fe_{20}}$	1.00	3.50	10.9	0.17–0.38	0.28(d)–0.33(b)
$\mathrm{Ni_{40}Fe_{10}Cu_{50}}$	0.50	1.92	1.41	0.14–0.26	(not known)

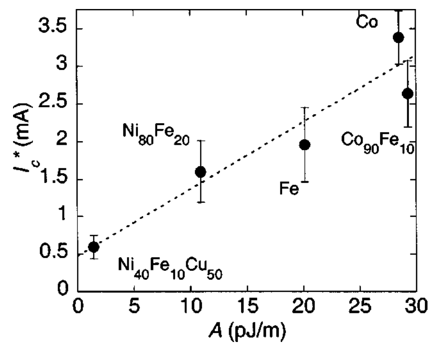

FIG. 3. Plot of I_c^* vs exchange energy density0 $A=M_sD/2\gamma\hbar$. The linear regression shown on the plot has $\chi^2=2.4$, which for three degrees of freedom is consistent with the hypothesis that the quantities are positively correlated.

$\rho_{\uparrow/\downarrow}$ and P, when available.[15,16] Given that the measured values for the efficiencies were determined using no free parameters, they are in reasonable agreement with predicted values, despite the large variations in the parameters M_s and D (also shown in Table I) over the range of materials. The efficiency is not strongly material-dependent; for the "typical" ferromagnetic materials measured (i.e., Fe, Co, $Co_{90}Fe_{10}$, and $Ni_{80}Fe_{20}$) there is little difference either expected or measured in ε.

A fraction of the contacts returned unphysically large efficiencies: $\varepsilon \gg 0.5$. As noted in Ref. 6, Eq. (1) assumes a certain rate of spin-wave radiation away from the tip. If spin-wave radiation is suppressed, for example, by a defect in or tip-induced damage to the film, the value of ε determined from the above analysis will be artificially large. Large values (>0.5) of ε occur in about 15% of the contacts.

Lower critical current values are desirable for applications. However, the data show that the average efficiency does not vary appreciably over the range of measured materials: Even use of a material with 100% polarization would increase ε (and reduce I_c) by less than a factor of two. On the other hand, Eq. (2) predicts that I_c should scale linearly with M_sD when $H_{app}=M_{eff}-H_{ex}$; that is, the applied field at which the net field on the magnetization is zero. The exchange energy density $A=M_sD/2\gamma\hbar$ varies by a factor of 10 over the materials studied, from 29.2 pJ/m for $Co_{90}Fe_{10}$ to 2.8 pJ/m for $Ni_{40}Fe_{10}Cu_{50}$.[17,18] Plotting the average $I_c^* \equiv I_c(H=M_s-H_{ex})$ versus A in Fig. 3, we find that I_c^* does indeed increase (by a factor of 5) over the range. The errors $\sigma_{\bar{x}}$ of the contact-to-contact variations in I_c^* are represented by the error bars.

To verify that the variations in I_c^* observed for a given material were not due to variations in the area from contact to contact, we performed a linear regression analysis on I_c^* versus the calculated contact area. This showed no correlation between I_c^* and the contact area when the area was estimated either from the contact resistance[19] or from the $I_c(H_{app})$ data by use of Eq. (1).[5] This is consistent with the somewhat unintuitive result that Eq. (2) is independent of contact area.[6] This independence is due to the balance of decreasing spin-wave radiation efficiency and increasing excitation volume with increasing contact size.

These results are consistent with Slonczewski's theory for describing the current-induced magnetic effects observed in these systems. With recent measurements definitively showing that spin-polarized dc currents induce precessional motion in field-biased magnetic layers,[7,8] these results suggest that the critical onset current for spin-torque-induced dynamics in multilayers can be varied over a wide range by adjusting M_s and D rather than only by employing materials with appreciably different spin polarizations.

This work supported in part by the DARPA SPinS programs. Contribution of NIST, not subject to copyright.

[1] J. A. Katine, F. J. Albert, R. A. Buhrman, E. B. Myers, and D. C. Ralph, Phys. Rev. Lett. **84**, 3149 (2000); F. B. Mancoff and S. E. Russek, IEEE Trans. Magn. **38**, 2853 (2002); E. B. Myers, D. C. Ralph, J. A. Katine, R. N. Louie, and R. A. Buhrman, Science **285**, 867 (1999); M. Tsoi, A. G. M. Jansen, J. Bass, W. C. Chiang, M. Seck, V. Tsoi, and P. Wyder, Phys. Rev. Lett. **80**, 4281 (1998); M. Tsoi, A. G. M. Jansen, J. Bass, W. C. Chiang, V. Tsoi, and P. Wyder, Nature (London) **406**, 46 (2000); J.-E. Wegrowe, A. Fábián, Ph. Guittienne, X. Hoffer, D. Kelly, J.-Ph. Ansermet, and E. Olive, Appl. Phys. Lett. **80**, 3775 (2002); J. Grollier, V. Cros, A. Hamzic, J. M. George, H. Jaffrès, A. Fert, G. Faini, J. Ben Youssef, and H. Legall, *ibid.* **78**, 3663 (2001).
[2] S. Urazhdin, N. O. Birge, W. P. Pratt, Jr., and J. Bass, cond-mat/0303149 v1.
[3] J. Z. Sun, D. J. Monsma, D. W. Abraham, M. J. Rooks, and R. H. Koch, Appl. Phys. Lett. **81**, 2202 (2002).
[4] J. Z. Sun, J. Magn. Magn. Mater. **202**, 157 (1999).
[5] W. H. Rippard, M. R. Pufall, and T. J. Silva, Appl. Phys. Lett. **82**, 1260 (2003).
[6] J. C. Slonczewski, J. Magn. Magn. Mater. **195**, L261 (1999).
[7] D. C. Ralph and R. A. Buhrman (unpublished).
[8] W. H. Rippard, M. R. Pufall, S. Kaka, S. E. Russek, and T. J. Silva (unpublished).
[9] S. S. P. Parkin suggested this technique for producing materials with different exchange stiffnesses.
[10] A. G. M. Jansen, A. P. van Gelder, and P. Wyder, J. Phys. C **13**, 6073 (1980), and references therein.
[11] K. Bussmann, G. A. Prinz, S. F. Cheng, and D. Wang, Appl. Phys. Lett. **75**, 2476 (1999); J. A. Katine, F. J. Albert, and R. A. Buhrman, *ibid.* **76**, 354 (2000).
[12] D. J. Monsma and S. S. P. Parkin, Appl. Phys. Lett. **77**, 883 (2000).
[13] R. J. Soulen, Jr., J. M. Byers, M. S. Osofsky, B. Naggorny, T. Ambrose, S. F. Cheng, P. R. Broussard, C. T. Tanaka, J. Nowak, J. S. Moodera, A. Barry, and J. M. D. Coey, Nature (London) **282**, 85 (1998).
[14] J. Bass and W. P. Pratt, J. Magn. Magn. Mater. **200**, 274 (1999).
[15] A. C. Reilly, W. Park, R. Slater, B. Ouaglal, R. Loloee, W. P. Pratt, and J. Bass, J. Magn. Magn. Mater. **195**, L269 (1999).
[16] S. Zhang and P. M. Levy, J. Appl. Phys. **69**, 4786 (1991).
[17] R. Bozorth, *Ferromagnetism* (IEEE, Piscataway, NJ, 1993), pp. 54, 112, 194, 265, and 156.
[18] C. Kittel, *Introduction to Solid State Physics*, 6th ed. (Wiley, NY, 1986), pp. 454.
[19] G. Wexler, Proc. Phys. Soc. London **89**, 927 (1966).